in: in: Atomic Processes in Plasmas, ed. E. Oks, M. Pindzola,
AIP Conf. Proc. 443 (1998)

Recoil Ion Momentum Spectroscopy
A 'momentum microscope' to view
atomic collision dynamics

R. Dörner[1], V. Mergel[1], H. Bräuning[1,2,3], M. Achler[1],
T. Weber[1], Kh. Khayyat[1], O. Jagutzki[1], L. Spielberger[1],
J. Ullrich[4], R. Moshammer[1,4], Y. Azuma[5], M.H. Prior[3],
C.L. Cocke[2], H. Schmidt-Böcking[1]

[1] *Institut für Kernphysik, Universität Frankfurt, August Euler Str. 6, D60486 Frankfurt, Germany*
[2] *Department of Physics, Kansas State University, Manhattan, KS 66506*
[3] *LBNL, Berkeley, CA 94720*
[4] *Fakultät für Physik, Universität Freiburg, Germany*
[5] *Photon Factory, IMSS, KEK, Tsukuba, Japan.*

Abstract. Recoil ion momentum spectroscopy is a powerful tool for investigating the dynamics of ion, electron or photon impact reactions with atoms or molecules. It allows to measure the three dimensional momentum vector of the ion from those reactions with high resolution and 4 π solid angle. It can be easily combined with novel 4 π electron momentum analysers and for coincident detection of the projectile. This technique gives a complete image of the square of the correlated many body final state wave function in momentum space (i.e. fully differential cross sections) for the various reactions. The application to photo double ionization of helium by linear and circular polarized light is discussed.

I INTRODUCTION

How do we understand a match on Center Court in Wimbledon? And what's necessary to enjoy a football game? To do so, two ingredients are indispensable. First, we need good detectors: Our eyes, or at least a TV camera, which can see the whole arena and deliver images bright and with high enough resolution to us so that we can follow the action of the players and the motion of the ball. And second, we need at least a rudimentary theory, i.e., the knowledge of some rules

of the game, to help us interpret what we see. These two ingredients open the way for a subtle interplay which enhances our understanding. Sometimes we learn the strategy of the game by carefully watching the players, and sometimes more detailed theoretical knowledge helps us to realize things we overlooked before. This article deals with only one side of the coin. It discusses a powerful camera to view the dynamics in the atomic collision arena. For the first time, an imaging technique called Cold Target Recoil Ion Momentum Spectroscopy (COLTRIMS) can give us a broad picture of atomic reactions in momentum space: capturing all aspects of the final state and providing bright, high resolution pictures of the breakup of atoms and molecules (see [1] for a recent review). Like a wide angle camera focused on the Center Court, it does not only show the motion of just one of the players, but captures the whole game with a resolution high enough that we can zoom in on any detail of interest. It delivers multi-dimensional momentum space images of the reaction, yielding the square of the many-body final state wave function.

One subfield of atomic physics has focused not on the dynamics in momentum space, but has achieved tremendous progress in the determination of energy eigenvalues. Laser spectroscopy, high resolution studies at synchrotron radiation sources, measurements in traps, dielectronic recombination studies and x-ray spectroscopy in ion storage rings provide us with unprecedented precise information on important quantities in atomic physics: energy levels and life times. These are time averaged quantities. They teach us the *static* long term properties of the atomic world. In the example of the tennis match, this corresponds to three-hour exposures of a photograph. It shows the probability distribution of the players on the court, like a time independent wave function in coordinate space which yields the eigenvalues. For observing a mountain or appreciating the beauty of a greek temple such long time exposures are clearly adequate, as they allow for extremely sharp pictures. For a tennis match, however, they obviously miss most of the fun. They will never tell us who won Wimbledon. Another very active subfield in atomic physics is working on unraveling the the basic many-body dynamics of atomic processes. Tremendous progress has been made here for example for (e,2e) and $(\gamma, 2e)$ reactions. Using coincident electron detection kinematically complete experiments could bee performed in this field (see eg. [2–9]. for $(\gamma, 2e)$ and [10–14] for (e,2e) and (e,3e)). Each of those experiments concentrates on certain angular or fragment energy ranges. Often a prohibitively large number of experiments would have to be performed to map the complete many particle momentum space. One of the fundamental technical challenges for fully differential experiments is the small solid angle of traditional spectrometers. The momentum space imaging techniques discussed in this paper are a concept to overcome this basic problem, by providing 4π solid angle for the coincident, three dimensional, high resolution momentum measurement of ions and electrons from atomic and molecular reactions.

The final state momenta of a reaction are interrelated by the three momentum and one energy conservation law. Thus for an n-body final state only 3n-4 momentum components have to be measured and the experimentalist is free to choose which to determine. For single ionization by fast charged particle impact for ex-

ample, the azimuthal and polar scattering angle of the projectile can be measured in coincidence with the three dimensional momentum vector of the recoil ion. The energy loss of the projectile and the momentum of the emitted electron can than be deduced using conservation laws. In many fast ion-atom collisions however the relative momentum change of the projectile (energy loss and scattering angle) is unmeasurable small (typically $\Delta p/p_{projectile} < 10^{-5}$). In this case a coincident momentum measurement of ion and electron(s) provides the only access to fully differential cross sections. The momenta are measured via combined position and time of flight (TOF) measurements. For the TOF either a pulsed beam or a coincidence with a projectile can be used. For photo double ionization, to give a second example, either the two electrons or one electron plus the ion can be measured. In this case again the easiest and most precise measurement can be performed if a pulsed beam enables an absolute TOF measurement of all particles. In some special cases however it is even sufficient to determine the relative time of flight between recoil ion and electron. The data for linear polarized light shown below are taken with a reference signal from a pulsed beam (see [15] for details on the timing), those for circular polarized light by only measuring the relative TOF (see [16]).

In the following we first briefly discuss the experimental technique and restrict ourself to discussing a few recent applications to low energy photo double ionization studies.

II EXPERIMENTAL TECHNIQUE

The basic principles for high resolution 4π spectrometers are identical for ion and electron detection. They are based on a small reaction volume (typically below 1 mm^3) from which the fragments are guided by electric and magnetic fields to large area position sensitive detectors. The momenta of electron and ion can then be calculated from the time of flight and the position where the particles hit the detectors. The ion momenta resulting from atomic reactions are typically in the range of a few atomic units (a.u.), their energies in the μeV - meV regime. This is comparable or even smaller than the thermal motion of the atoms at room temperature (4.6 a.u. for He). Thus, one has to provide an internally cold atomic target for the collision. This is presently achieved by using supersonic gas jet targets. A further improvement in resolution is envisaged by the future use of laser cooled targets [17].

In all high resolution collision COLTRIMS studies supersonic gas jet targets have been used. The gas jet is formed by expanding the gas through a 30 μm hole. In some cases the nozzle and the gas are precooled to 15-30 K to further improve the resolution. From this expansion a supersonic jet is formed and the He atoms have a mean speed proportional to the square root of the nozzle temperature. The momentum distribution around the mean value is given by the speed ratio of the expansion [19]. The precooling helps to achieve a narrow momentum distribution

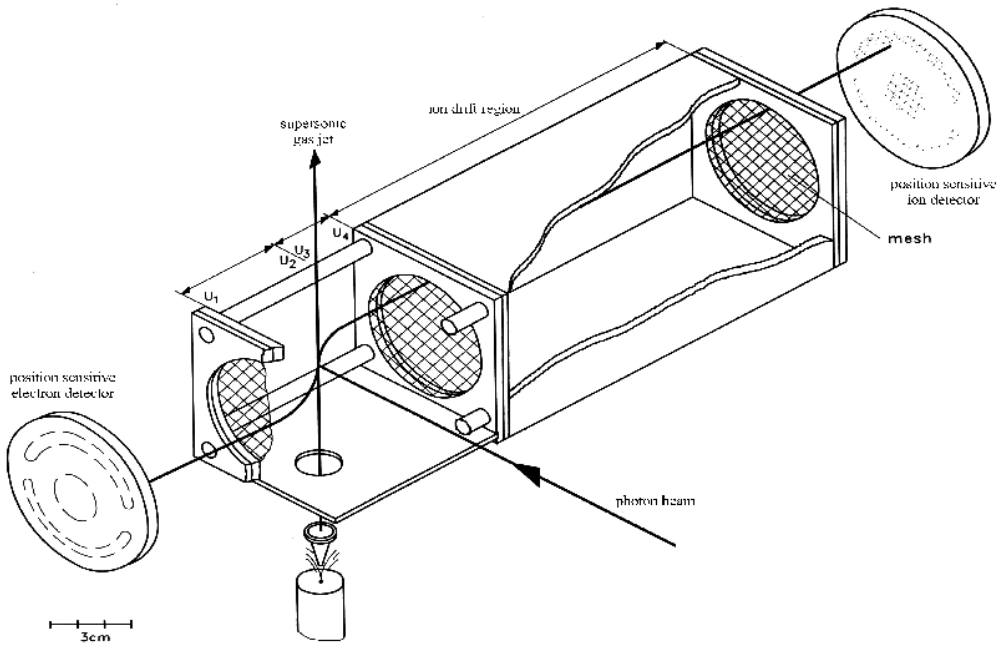

FIGURE 1. Typical COLTRIMS setup. The gas nozzle is cooled to 15-30 K, the super sonic gas jet has a diameter of 1.1 mm at the intersection with the photon (or charged particle) beam. The electron detector is located on the left side of the spectrometer and the ion detector on the right side. (from [18])

with small turbo pumps. About 1 cm above the nozzle the inner part of the preformed gas jet enters the scattering chamber through a skimmer of 0.3 mm diameter. A typical operating condition for precooled one stage jets with small turbo pumps is a driving pressure of 400 mbar. This results in 5×10^{-4} mbar in the source chamber and a local target pressure of a few 10^{-5} mbar at the target region, 3 cm above the skimmer. The gas jet leaves the scattering chamber into a separately pumped jet dump. In other experiments two stage jets [20,21] or jets backed with 8000 l/s diffusion pumps [22,23] are successfully used.

The ions are created in the overlap volume of the gas jet with the projectile beam. Different designs for recoil ion and electron spectrometers have been used. In a first version a homogeneous electric field followed by a drift tube guided the ions to a position sensitive channel plate [24–29]. With this homogeneous field spectrometer Mergel and coworkers reported a resolution of 0.26 a.u. [25]. A very flexible combination of electric fields for ion detection and magnetic fields for guiding the electrons has been used at GSI [30–34]. This 'momentum microscope' is discussed in detail in [21]. In all spectrometers with homogeneous fields the ion momentum resolution is restricted by the extension of the overlap volume. To circumvent this restriction Mergel [18] has designed a field geometry which is focussing in three

dimensions. An electrostatic lens in the extraction region focuses different starting positions perpendicular to the extraction field onto one point on the detector. In the third direction different starting points along the field lead to the same time of flight. Thus, a high resolution can be achieved even with a gas target extended over several mm. With this spectrometer a resolution of 0.07 a.u FWHM, which is close to the internal temperature of the gas jet, has been reached [35]. Details on the field geometry can be found in [15,18]. A typical COLTRIMS setup is shown in figure 1.

Due to the low energy of the recoiling ions a moderate field of a few V/cm is sufficient to collect all ions onto the detector. The same field is used to guide the electrons in the opposite direction. If one chooses a distance of 2 cm from the target region to the electron detector a 4π collection efficiency can be reached only for very low energy electrons (1-5 eV). In fast particle collisions however often higher energy electrons are created. To guide such electrons to the detector Moshammer and coworkers have superimposed on the electric field a homogenous magnetic field yielding 4π detection efficiency up to 30 eV electron energy [21]. Higher electron energies can be accessed by increasing the magnetic and electric fields. Such electron imaging spectrometers with magnetic confinement are used with great success in ion impact [30,33,32,21,34] and in photo ionization studies [36,37].

III APPLICATION TO PHOTO IONIZATION STUDIES

A particular interesting case of an atomic few body reaction is double ionization of He by one single photon. This process is a detailed probe of the effects of dynamic electron correlation, one of the hottest topics in todays atomic collision physics. The most simple and widely studied quantity for this reaction is the ratio of total cross sections for double to single ionization (see eg the recent experimental papers [38–41]). For a detailed understanding of the dynamics however much higher differential cross sections are needed.

Starting with the pioneering work of Schwarzkopf and coworkers in 1993 [2] several groups have reported electron coincidence studies for He double double ionization [3–9]. These experiments have covered several angular settings between the electron spectrometers as well as equal and unequal sharing of the excess energy available to the system. They have however been restricted to the coplanar geometry, where the two electrons move in a plane containing the polarization vector of the linear polarized light.

As outlined in the introduction, detecting the momentum vector of the He^{2+} ion and one of the electrons is equivalent to detecting both electrons in coincidence. Several studies [42,43,36,15,16] reported on such experiments which mostly cover the full momentum space of all particles. One of the major advantages of such a comprehensive data set for double ionization is the possibility to display the data in any set of coordinates. Thus not only the traditional angles and energies of the

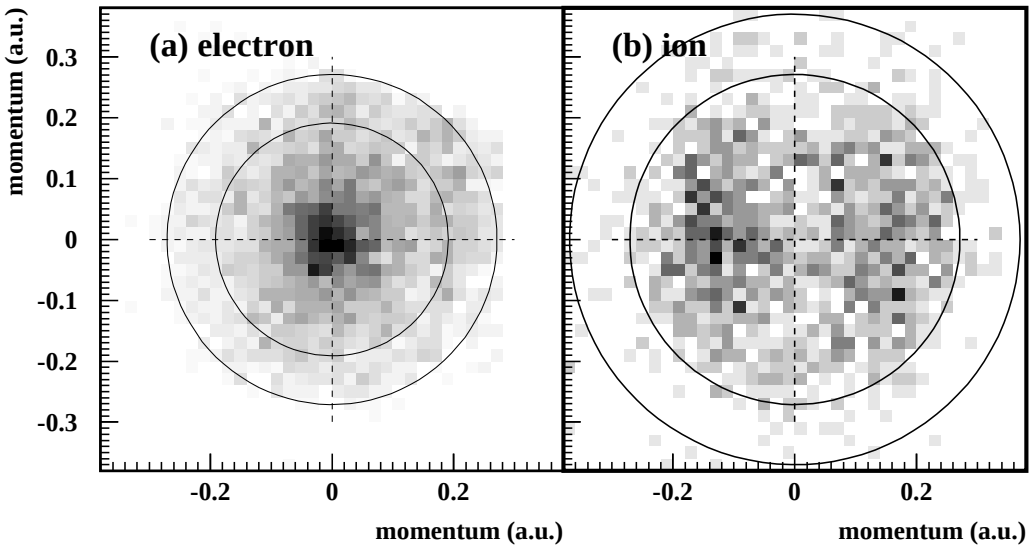

FIGURE 2. Density plots of projections of the momentum distribution from double ionization of He by 80.1 eV linear polarized photons. The z and y components of the momentum are plotted on the horizontal and vertical axes, respectively. The polarization vector of the photon is in the z direction and the photon propagates in the x direction. Only events with -0.1< k_{rx} <0.1 a.u. are projected onto the plane. a) The distribution of single electron momenta ($\mathbf{k_1}$ or $\mathbf{k_2}$). The circle locates the momentum of an electron which carries the full excess energy. (b) The recoil (or $-\mathbf{k_r}$) momentum distribution. The outer circle indicates the maximum calculated recoil momentum, and the inner circle is the locus of events for which the $\mathbf{k_r}$ motion has half of the excess energy (from [42]).

two electrons (or momenta $\mathbf{k_1}, \mathbf{k_2}$) can be chosen but also collective coordinates like Jacobi coordinates ($\mathbf{k_r} = \mathbf{k_1} + \mathbf{k_2}$ and $\mathbf{k_R} = \mathbf{1/2}(\mathbf{k_1} - \mathbf{k_2})$) or hyperspherical coordinates. In such momentum space images the characteristics of the photo double ionization process become directly visible. Figure 2 compares a two dimensional representation of the final state momentum distribution of the He^{2+} ion and one of the electrons. The nucleus clearly shows a dipolar emission pattern as a result of the absorption of the photon. This characteristics of the primary absorption process is completely washed out in the electronic momentum distribution. This highlights the fact, that the nucleus as the center of positive charge in the system always participates in the absorbtion of the photon. It is the electron electron interaction which always is required in order for double ionization which smears out this reminiscent of the photons angular momentum in the momentum distribution of one single electron. A more detailed discussion of this problem can be found in [42,44,45,36].

An overview of the three body continuum in the momenta of the two electrons is given in figure 3. It shows the momentum of one electron with respect to the

other at 1 and 20 eV above the double ionization threshold. All three particles are necessarily in one plane (following from momentum conservation). This internal plane of the breakup has some orientation to the electric field vector ϵ of the linear polarized photon beam.

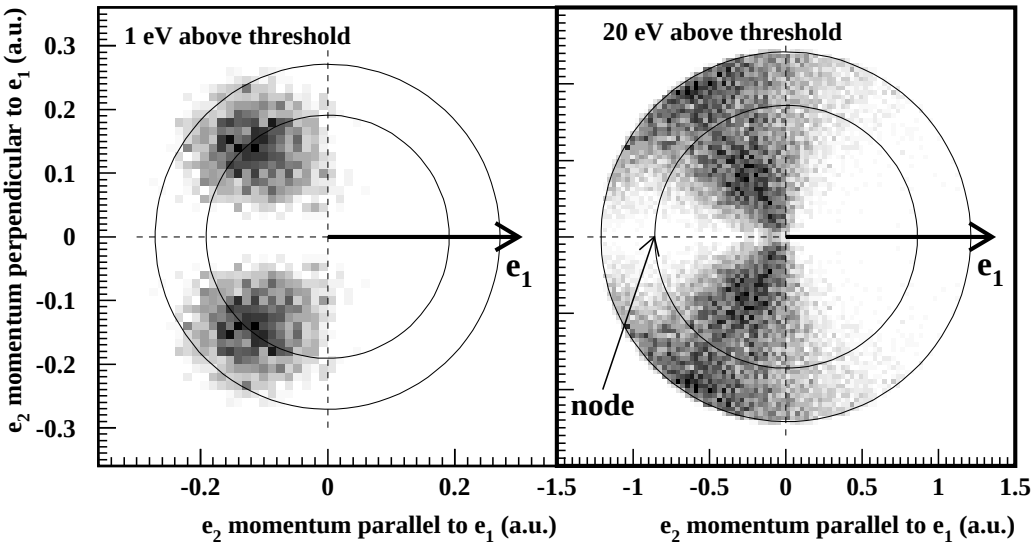

FIGURE 3. Photo double ionization of He at 1 and 20 eV above threshold by linear polarized light. Shown is the momentum distribution of electron 2 for fixed direction of electron 1 as indicated. The plane of the figure is the internal momentum plane of the three particles. The data are integrated over all orientations of the polarization axis with respect to this plane. The figure thus samples the full cross sections, all angular and energy distributions of the fragments. The outer circle corresponds to the maximum possible electron momentum, the inner one to the case of equal energy sharing. (see text for details)

In the figure we show the momenta of the electrons in this internal plane integrated over all directions of ϵ. Electron 1 is chosen along the positive x axis of the figure (shown by the arrow). The full cross section, all energy sharings and all angles, are sampled in this figure. Each circle on this plane corresponds to a particular energy sharing. The outer circle gives the maximum available momentum (i.e. extremely unequal energy sharing), the inner circle corresponds to equal energy sharing. As has been shown already by the work using coincident electron detection (see e.g.
citeSchwarzkopf93,Schwarzkopf94,Schwarzkopf95jpb,Huetz94, two main features determine the momentum distribution: the effect of electron repulsion and a selection rule from the $^1P^0$ symmetry of the final state. Electron repulsion at these low excess energies leads to an emission of the electrons to opposite half spheres. There are almost no events on the right half of the figure corresponding to two electrons going to the same internal half plane. As can be expected from the velocity of the

particles, this backward emission effect is slightly more pronounced at 1 eV than at 20 eV. Second, for a $^1P^0$ two body state $\mathbf{k_1} = -\mathbf{k_2}$, i.e. back to back emission of equal energy electrons, is prohibited (see selection rule C in [46]). For 1 eV the data show that this node extends all the way along the x-axis. Thus at such low energies back to back emission is suppressed at all energy sharings, even so this is not a strict selection rule (see also [7]). At 20 eV the node is really centered at $\mathbf{k_1} = -\mathbf{k_2}$ (indicated by the arrow). This presentation shows strikingly that this node is internal to the three body system and has nothing to do with ϵ, since the data are integrated over all orientations of ϵ.

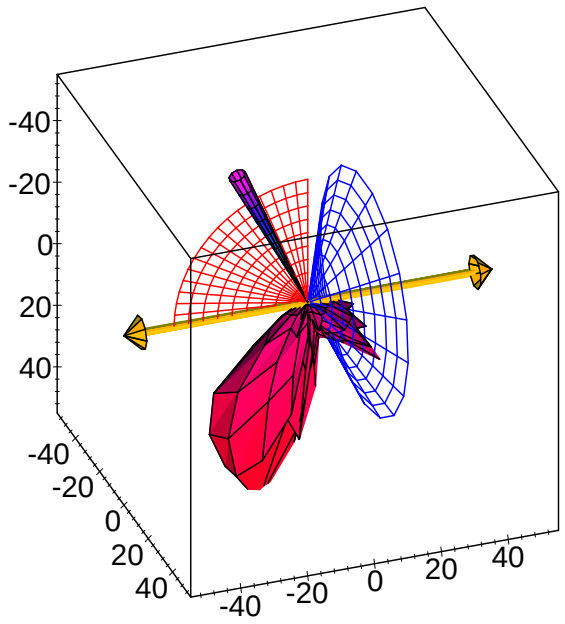

FIGURE 4. Four fold differential cross section $d^4\sigma/d\vartheta_1 d\vartheta_2 d\Phi_{1-2} dE_1$ The direction of the slow electron is indicated by the narrow dark cone (at ϑ_1 =65 deg), the polarization is horizontal, indicated by the double arrow. The excess energy is 6 eV, the fixed electron has 0.1-1 eV

An additional structure becomes visible if one avoids this integration and displays the data in the conventional polar coordinates. Figure 4 shows the fourfold differential cross section $d^4\sigma/d\vartheta_1 d\vartheta_2 d\Phi_{1-2} dE_1$ at 6 eV. Strictly speaking this is a fivefold differential cross section, since the are five linear independent observables. Within the dipol approximation, the additional rotational symmetry around the polarization axis reduces this to four dimension. The direction of the first electron is indicated by the narrow cone. The polarization axis is horizontal. The wide open cone on the right represented by the mesh indicates the locus of a two-dimensional node according to selection rule F of [46]. This selection rule holds strictly only for equal energy sharing. As the data show at 6 eV excess energy it prevails however for unequal energy sharing (see [15,6,7]).

An interesting twist is added to this three body breakup if one introduces a chirality in the initial state by inducing the transition with circular instead of linear polarized light. The question arises how or if at all the chirality of the photon is transferred to the three body continuum. It has been first pointed out by Berakdar and Klar [47] that such an effect, termed dichroism, might exist even for He double ionization. Viefhaus and coworkers [9] found the first experimental evidence for this effect. The two electrons and the photon axis can span a tripod which could have a handedness if its two legs defined by the electron momenta are distinguishable, i.e. the electrons have unequal energy. This shows up strongest if the three body plane (as it is shown in figure 3) is held fix perpendicular to the photon axis. At 20 eV above threshold, figure 5 shows the momentum distribution of the ion and electron 2 in this plane. The momentum of electron 1,which is chosen to be the faster one, is fixed along the x axis.

Comparison with figure 3 as well as between left and right circular polarized light visualizes that dichroism is a huge effect in this system. While for linear polarized light upper and lower half of the figure are necessarily symmetric, this symmetry is broken for circular polarized light. A detailed comparison of these experimental results with 3C calculations can be found in [16]. In general the agreement between 3C theory and experiment is much worse for circular polarized [16] than for linear polarized light.

IV OUTLOOK

Multiparticle imaging with COLTRIMS provides new spectacular views on many body breakup of coulombic systems. It combines high resolution in momentum space (typically $<< 0.1 a.u.$) with 4π solid angle for all fragments. In many cases such kinematical complete pictures directly 'display' the processes responsible for the breakup of the atom or molecule. Thus some long standing puzzles in atomic collision physics were solved recently using this approach and many new questions and challenges to theory were raised. Due to limited space we had to restrict ourselves to a few selected results for photoionization at low energies. Another rich field of applications lies in the study of Compton scattering at high photon energies [23,41]. A great amount of important results could be obtained in particular for ion atom collisions. We name only a few of these: Momentum space of single and double ionization by relativistic heavy ions showed the explosion of the atom in the light of an attosecond pulse of virtual photons, stronger than any available laser [33,32,30]. A scattering of two electrons inside an atom in a transfer ionization process could be directly seen [48]. Two center electron-electron interaction has been separated experimentally from nuclear-electron scattering [49,27]. At slow collisions the promotion of one electron into the continuum via the saddle point mechanism has been imaged [50,51]. Besides this rapidly increasing progress in atomic and molecular [37] physics such imaging techniques can be expected to be particularly useful in material research and solid state physics in the future. On

can envision even the imaging of the many electron emission from surfaces which will give insight in the correlated electron motion in solids.

V ACKNOWLEDGEMENTS

The work was financially supported by DFG, BMFT and by the Division of Chemical Sciences, Basic Energy Sciences, Office of Energy Research, U.S.Department of Energy, DOE grant 82ER53128 (KSU) and DOE contract No. DE-AC03-76SF00098 (LBNL). One of us (R.D.) was supported was supported by the Habilitanden Programm der DFG. H.B. and R.D. acknowledge support from the Alexander von Humboldt foundation. Kh. K. greatfully acknowledges support by the DAAD. We also acknowledge financial support from Max Planck Forschungspreis of the Humboldt foundation. The work presented for linear polarized light would not have been possible without the great support at the ALS in particular by R. Thatcher, T. Warwick, E. Rothenberg and J. Dennlinger. For the data with circular polarized light we acknowledge the help of Dr. T. Hatano and Prof. T. Miyahara and the excellent working conditions at the Photon Factory during the experiment (Proposal No. 96G160) and of T. Kambara, V. Zoran, Y. Awaya and B. Nystrom doe their help during the beamtime. The interpretation of the photo ionization data profited from many discussions with our friends and colleagues J. Feagin, S. Keller, J. Berakdar, V. Schmidt, B. Kässig, C. Wheelan and A. Huetz.

REFERENCES

1. J. Ullrich, R. Moshammer, R. Dörner, O. Jagutzki, V. Mergel, H. Schmidt-Böcking, and L. Spielberger. *J. Phys*, B30:2917, 1997. *Topical Review.*
2. O. Schwarzkopf, B. Krässig, J. Elmiger, and V. Schmidt. *Phys. Rev. Lett.*, 70:3008, 1993.
3. O. Schwarzkopf, B. Krässig, V. Schmidt, F. Maulbetsch, and J. Briggs. *J. Phys.*, B27:L347–50, 1994.
4. O. Schwarzkopf and V. Schmidt. *J. Phys.*, B28:2847, 1995.
5. A. Huetz, P. Lablanquie, L. Andric, P. Selles, and J. Mazeau. *J. Phys.*, B27:L13, 1994.
6. G. Dawber, L. Avaldi, A.G. McConkey, H. Rojas, M.A. MacDonald, and G.C. King. *J. Phys.*, B28:L271, 1995.
7. P. Lablanquie, J. Mazeau, L. Andric, P. Selles, and A. Huetz. *Phys. Rev. Lett.*, 74:2192, 1995.
8. J. Viefhaus, L. Avaldi, F. Heiser, R. Hentges, O. Gessner, A. Rüdel, M. Wiedenhöft, K. Wielczek, and U. Becker. *J. Phys.*, B29:L729, 1996.
9. J. Viefhaus, L. Avaldi, G. Snell, M. Wiedenhöft, R. Hentges, A. Rüdel, F. Schäfer, D. Menke, U. Heinzmann, A. Engelns, J. Berakdar, H. Klar, and U. Becker. *Phys. Rev. Lett.*, 77:3975, 1996.

10. M.A. Coplan et al. *Rev.Mod.Phys.*, 66:985, 1994, and References therein.
11. I.E. McCarthy and E. Weigold. *Rep. Prog. Phys.*, 54:789, 1991.
12. A. Lahmam-Bennani. *J. Phys*, B24:2401, 1991.
13. B. El Marji, A. Lahmam-Bennani, A. Duguet, and T.J. Reddish. *J. Phys*, B29:L1, 1996.
14. B. El Marji, C. Schröter, A. Duguet, A. Lahmam-Bennani, M. Lecas, and L. Spielberger. *J. Phys*, B30:3677, 1997.
15. R. Dörner, H. Bräuning, J.M. Feagin, V. Mergel, O. Jagutzki, L. Spielberger, T. Vogt, H. Khemliche, M.H. Prior, J. Ullrich, C.L. Cocke, and H. Schmidt-Böcking. *Phys. Rev.*, A57:1074, 1998.
16. V.Mergel, M. Achler, R. Dörner, Kh. Khayyat, T. Kambara, Y. Awaya, V. Zoran, B. Nyström, L.Spielberger, J.H. McGuire, J. Feagin, J. Berakdar, Y. Azuma, , and H. Schmidt-Böcking. *Phys. Rev. Lett.*, 80:5301, 1998.
17. S. Wolf and H. Helm. *Phys. Rev.*, A56:R4385, 1997. .
18. V. Mergel. PhD thesis*, Universität Frankfurt*. ISBN 3–8265–2067–X. Shaker Verlag, 1996.
19. G. Brusdeylins, J.P. Toennies, and R. Vollmer. page 98, Perugia, 1989.
20. P. Jardin, J.P. Grandin, A. Cassimi, J.P. Lemoigne, A. Gosseling, X. Husson, D. Hennecart, and A. Lepoutre. In *AIP Conference Proceedings No 274*, page 291. AIP, 1993.
21. R. Moshammer, M. Unverzagt, W. Schmitt, J. Ullrich, and H. Schmidt-Böcking. *Nucl. Instr. Meth.*, B 108:425, 1996.
22. O. Jagutzki, L. Spielberger, R. Dörner, S. Nüttgens, V. Mergel, H. Schmidt-Böcking, J. Ullrich, R.E. Olson, and U. Buck. *Zeitschrift für Physik*, D36:5, 1996.
23. L. Spielberger, O. Jagutzki, R. Dörner, J. Ullrich, U. Meyer, V. Mergel, M. Unverzagt, M. Damrau, T. Vogt, I. Ali, Kh. Khayyat, D. Bahr, H.G. Schmidt, R. Frahm, and H. Schmidt-Böcking. *Phys. Rev. Lett.*, 74:4615, 1995.
24. O. Jagutzki. *Dissertation Unversität Frankfurt*, unpublished, 1994.
25. V. Mergel, R. Dörner, J. Ullrich, O. Jagutzki, S. Lencinas, S. Nüttgens, L. Spielberger, M. Unverzagt, C.L. Cocke, R.E. Olson, M. Schulz, U. Buck, E. Zanger, W. Theisinger, M. Isser, S. Geis, and H. Schmidt-Böcking. *Phys. Rev. Lett.*, 74:2200, 1995.
26. V. Mergel. *Diploma thesis Universität Frankfurt*, unpublished, 1994.
27. R. Dörner, V. Mergel, R. Ali, U. Buck, C.L. Cocke, K. Froschauer, O. Jagutzki, S. Lencinas, W.E. Meyerhof, S. Nüttgens, R.E. Olson, H. Schmidt-Böcking, L. Spielberger, K. Tökesi, J. Ullrich, M. Unverzagt, and W. Wu. *Phys. Rev. Lett.*, 72:3166, 1994.
28. R. Dörner, V. Mergel, L. Zhaoyuan, J. Ullrich, L. Spielberger, R.E. Olson, and H. Schmidt-Böcking. *J. Phys*, B28:435, 1995.
29. V. Mergel, R. Dörner, J. Ullrich, O. Jagutzki, S. Lencinas, S. Nüttgens, L. Spielberger, M. Unverzagt, C.L. Cocke, R.E. Olson, M. Schulz, U. Buck, and H. Schmidt-Böcking. *Nucl. Instr. Meth.*, B96:593, 1995.
30. R. Moshammer, J. Ullrich, M. Unverzagt, W. Schmidt, P. Jardin, R.E. Olson, R. Mann, R. Dörner, V. Mergel, U. Buck, and H. Schmidt-Böcking. *Phys. Rev. Lett.*, 73:3371, 1994.

31. M. Unverzagt, R. Moshammer, W. Schmitt, R.E. Olson, P. Jardin, V. Mergel, J. Ullrich, and H. Schmidt-Böcking. *Phys. Rev. Lett.*, 76:1043, 1996. .
32. R. Moshammer, J. Ullrich, H. Kollmus, W. Schmitt, M. Unverzagt, O. Jagutzki, V. Mergel, H. Schmidt-Böcking, R. Mann, C.J. Woods, and R.E. Olson. *Phys. Rev. Lett.*, 77:1242, 1996.
33. R. Moshammer, J. Ullrich, W. Schmitt, H. Kollmus, A. Cassimi, R. Dörner, R. Dreizler, O. Jagutzki, S. Keller, H.-J. Lüdde, R. Mann, V. Mergel, R.E. Olson, T. Prinz, H.Schmidt-Böcking, and L Spielberger. *Phys. Rev. Lett.*, 79:3621, 1997.
34. R. Moshammer, J. Ullrich, H. Kollmus, W. Schmitt, M. Unverzagt, H.Schmidt-B"ocking, C.J. Wood, and R.E. Olson. *Phys. Rev.*, A56:1351, 1997.
35. R. Dörner, V. Mergel, L. Spielberger, O. Jagutzki, S. Nüttgens, M. Unverzagt, H. Schmidt-Böcking, J. Ullrich, R.E. Olson, K. Tökesi, W.E. Meyerhof, W. Wu, and C.L. Cocke. *AIP Conf. Proc. 360 (1995) Editors: L.J. Dube, J.B.A. Mitchell J.W. McConckey C.E. Brion*, AIP Press New York, 1995.
36. H.P Bräuning, R. Dörner, C.L. Cocke, M.H. Prior, B. Krässig, A. Bräuning-Demian, K. Carnes, S. Dreuil, V. Mergel, P. Richard, J. Ullrich, and H. Schmidt-Böcking. *J. Phys.*, B30:L649, 1997.
37. R. Dörner, H. Bräuning, O. Jagutzki, V. Mergel, M. Achler, R. Moshammer, J. Feagin, A. Bräuning-Demian, L. Spielberger, J.H. McGuire, M.H. Prior, N. Berrah, J. Bozek, C.L. Cocke, and H. Schmidt-Böcking. *Phys. Rev. Lett.*, 81:5776, 1998.
38. J.A.R. Samson, W.C. Stolte, Z.X. He, J.N. Cutler, Y. Lu, and R.J. Bartlett. *Phys. Rev.*, A57:1906, 1998.
39. R. Dörner, T. Vogt, V. Mergel, H. Khemliche, S. Kravis, C.L. Cocke, J. Ullrich, M. Unverzagt, L. Spielberger, M. Damrau, O. Jagutzki, I. Ali, B. Weaver, K. Ullmann, C.C. Hsu, M. Jung, E.P. Kanter, B. Sonntag, M.H. Prior, E. Rotenberg, J. Denlinger, T. Warwick, S.T. Manson, and H. Schmidt-Böcking. *Phys. Rev. Lett.*, 76:2654, 1996.
40. J. C. Levin, G. B. Armen, and I. A. Sellin. *Phys. Rev. Lett.*, 76:1220, 1996.
41. L. Spielberger, O. Jagutzki, B. Krässig, U. Meyer, Kh. Khayyat, V. Mergel, Th. Tschentscher, Th. Buslaps, H. Bräuning, R. Dörner, T. Vogt, M. Achler, J. Ullrich, D.S. Gemmel, and H. Schmidt-Böcking. *Phys. Rev. Lett.*, 76:4685, 1996.
42. R. Dörner, J. Feagin, C.L. Cocke, H. Bräuning, O. Jagutzki, M. Jung, E.P. Kanter, H. Khemliche, S. Kravis, V. Mergel, M.H. Prior, H. Schmidt-Böcking, L. Spielberger, J. Ullrich, M. Unverzagt, and T. Vogt. *Phys. Rev. Lett.*, 77:1024, 1996. see also erratum in Phys. Rev. Lett. 78. 2031 (1997).
43. T. Vogt, R. Dörner, O. Jagutzki, C.L. Cocke, J. Feagin, M. Jung, E.P. Kanter, H. Khemliche, S. Kravis, V. Mergel, L. Spielberger, J. Ullrich, M. Unverzagt, H. Bräuning, U. Meyer, and H. Schmidt-Böcking. *in: Proceedings of the Euroconference Ionization and Coincidence Spectroscopy ed.: C.T. Whelan and H.R.J. Walters, Plenum, 1997.*
44. M. Pont and R. Shakeshaft. *Phys. Rev.*, A54:1448, 1996.
45. J.M. Feagin. *J. Phys.*, B29:l551, 1996.
46. F. Maulbetsch and J.S. Briggs. *J. Phys.*, B28:551, 1995.
47. J. Berakdar and H. Klar. *Phys. Rev. Lett.*, 69:1175, 1992.
48. V. Mergel, R. Dörner, M. Achler, Kh. Khayyat, S. Lencinas, J. Euler, O. Jagutzki,

S. Nüttgens, M. Unverzagt, L. Spielberger, W. Wu, R. Ali, J. Ullrich, H. Cederquist, A. Salin, R.E. Olson, Dž. Belkić, C.L. Cocke, and H. Schmidt-Böcking. *Phys. Rev. Lett.*, 79:387, 1997.
49. W. Wu, R. Ali, C.L. Cocke, V. Frohne, J.P. Giese, B. Walch, K.L. Wong, R. Dörner, V. Mergel, H. Schmidt-Böcking, and W.E. Meyerhof. *Phys. Rev. Lett.*, 72:3170, 1994.
50. S.D. Kravis, M. Abdallah, C.L. Cocke, C.D. Lin, M. Stöckli, B. Walch, Y. Wang, R.E. Olson, V.D. Rodriguez, W. Wu, M. Pieksma, and N. Watanabe. *Phys. Rev.*, A54:1394, 1996.
51. R. Dörner, H. Khemliche, M.H. Prior, C.L. Cocke, J.A. Gary, R.E. Olson, V. Mergel, J. Ullrich, and H. Schmidt-Böcking. *Phys. Rev. Lett.*, 77:4520, 1996.

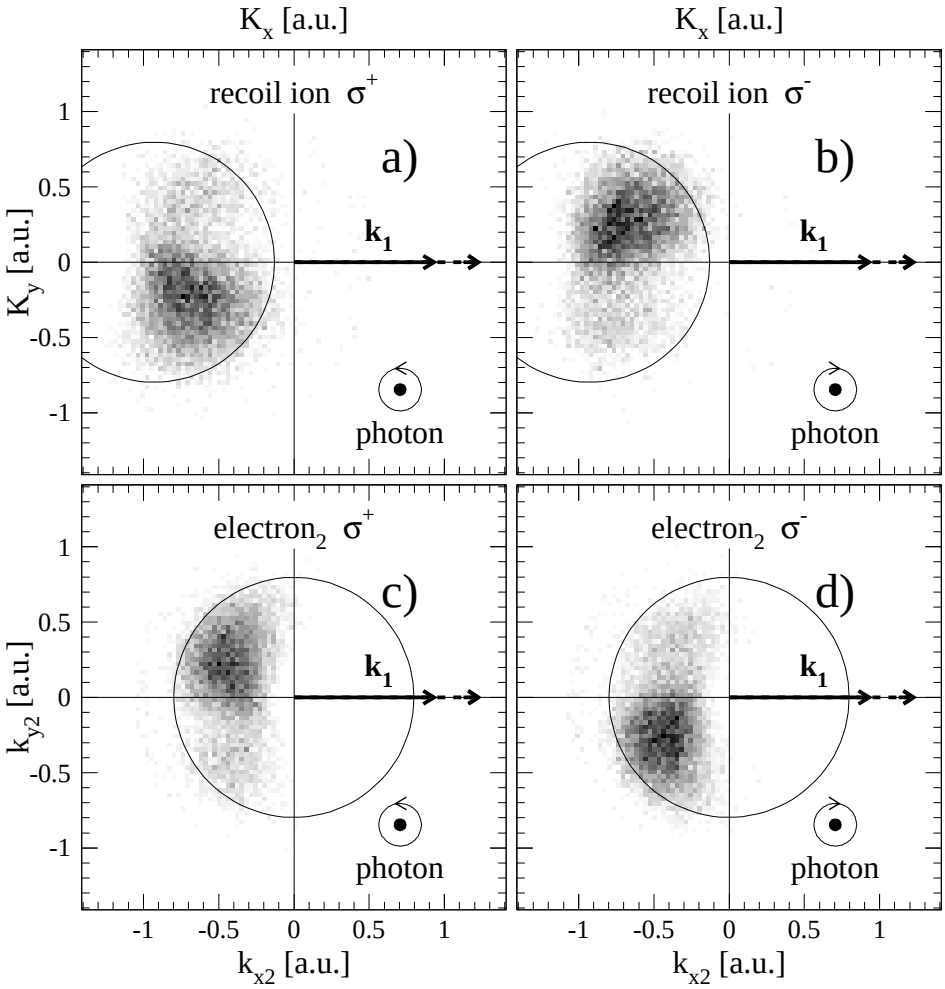

FIGURE 5. Recoil ion and electron momentum distribution in the x-y-plane both for σ^+ and σ^- as indicated. We fixed e_1 within 0.9a.u. $< k_{x1} <$ 1.2a.u. and with $k_{y1} = k_{z1} = 0$. The wave vector $\mathbf{k}_\gamma$ points out of the plane of paper. Circles: maximum magnitude of $\mathbf{K}$ and $\mathbf{k}_2$. The grey scale represents the five fold differential cross section on a linear scale (from [16]).